JASN Express. Published on January 3, 2007 as doi: 10.1681/ASN.2006050501

Pkd2$^{+/-}$ Vascular Smooth Muscles Develop Exaggerated Vasocontraction in Response to Phenylephrine Stimulation

Qi Qian,*† Larry W. Hunter,† Hui Du,* Qun Ren,* Young Han,† and Gary C. Sieck†

**Division of Nephrology and Hypertension, †Department of Physiology and Biomedical Engineering, Mayo Clinic College of Medicine, Rochester, Minnesota*

Vascular complications are the leading cause of morbidity and mortality in autosomal dominant polycystic kidney disease. Although evidence suggests an abnormal vascular reactivity, contractile function in *Pkd* mutant vessels has not been studied previously. Contractile response to phenylephrine (PE; 10^{-10} to 10^{-4}M), an α1-adrenergic receptor agonist, was examined. De-endothelialized *Pkd2*$^{+/-}$ aortic rings generated a higher maximum force (F_{max}) than that in wild-type (wt; 5.78 ± 0.73 *versus* 2.69 ± 0.43 mN; $P < 0.001$) and a significant left shift in PE dosage-response curve. On simultaneous recordings, *Pkd2*$^{+/-}$ aortic helical strips also responded to PE with a greater F_{max} but a lesser $[Ca^{2+}]_i$ rise, resulting in a greatly enhanced Δforce/ΔCa^{2+} ratio than that in wt. At F_{max}, a higher elevation in the phosphorylated regulatory myosin light chain was observed in *Pkd2*$^{+/-}$ strips. Ca^{2+}-dependent calmodulin/myosin light-chain kinase–mediated contraction was examined by direct Ca^{2+} (pCa8-5) stimulation to β-escin permeabilized aortic strips; the pCa-force curve in *Pkd2*$^{+/-}$ strips was not shifted, thereby indicating that PE induced dosage-response alteration that resulted from Ca^{2+}-independent mechanisms. Quantitative analyses of contractile proteins demonstrated elevated expressions in smooth muscle α-actin and myosin heavy chain in *Pkd2*$^{+/-}$ arteries, changes that likely contribute to the higher F_{max}. Similar to those in aortas, de-endothelialized *Pkd2*$^{+/-}$ resistance (fourth-order mesenteric) arteries responded to PE with a stronger contraction but a lesser $[Ca^{2+}]_i$ rise than in wt. Taken together, the arterial vasculature in *Pkd2*$^{+/-}$ mice exhibits an exaggerated contractile response and increased sensitivity to PE. An enhanced Ca^{2+}-independent force generation and elevated contractile protein expression likely contribute to these abnormalities.

J Am Soc Nephrol 18: ●●●–●●●, 2007. doi: 10.1681/ASN.2006050501

Autosomal dominant polycystic kidney disease (ADPKD) is caused by mutations to the *PKD1* or *PKD2* gene. The leading cause of morbidity and mortality in ADPKD is vascular disease, the latter comprising hypertension, intracranial aneurysms/aneurysmal rupture, thoracic aortic dissection, renal vasoconstriction, and intracranial arterial vasospasm (1–5). Mice with targeted *Pkd* mutations likewise exhibit significant vascular abnormalities. *Pkd1*$^{-/-}$ or *Pkd2*$^{-/-}$ mutation causes lethal cardiac defects and vascular hemorrhages (6,7). *Pkd1*$^{+/-}$ mutation or a reduced expression of polycystin-1 (the gene product of *Pkd1*) is associated with hypertension (8) and dissecting aortic aneurysms (9). *Pkd2*$^{+/-}$ mutation is associated with a reduced tolerance to hemodynamic stress and a shorter life expectancy independent of renal dysfunction (10,11). These observations demonstrate that *PKD* (human)/*Pkd* (mice) mutations predispose to assorted derangements in the vasculature, including a propensity to a heightened vasocontraction.

Vasocontraction is generated *via* cyclic interactions/movements between the thick and thin contractile filaments, which are composed of smooth muscle myosin heavy chain (SM MHC; the molecular motor) and SM α-actin, respectively, in vascular smooth muscle cells (VSMC). The key regulation to vasocontraction lies in the phosphorylation of the regulatory myosin light chain (MLC_{20}). When phosphorylated, MLC_{20} (bound noncovalently to SM MHC) changes the structural conformation of SM MHC and permits its binding to ATP and α-actin, leading to actomyosin cross-bridge formation and actin-activated ATPase activation (by approximately 700-fold). The ensuing ATP hydrolysis releases energy to generate power stroke (force). MLC_{20} phosphorylation triggers a cascade of events that ultimately convert chemical energy to mechanical contraction (12).

The net level of phosphorylated MLC_{20} is determined by the activity ratio of MLC_{20} kinase to phosphatase. The activities of the kinases/phosphatase can be modulated in a Ca^{2+}-dependent or Ca^{2+}-independent manner. MLC_{20} kinases include Ca^{2+}/calmodulin (CaM)-dependent myosin light-chain kinase (MLCK) or Ca^{2+}-independent ILK and ZIPK (13,14), whereas MLC_{20} phosphatase (SMPP-1M) is Ca^{2+} independent (15). A number of well-studied vasocontractive stimulators, including phenylephrine (PE; a α1-adrenergic receptor [α1-AR] agonist), raises cellular phosphorylated MLC_{20} *via* both Ca^{2+}/CaM-dependent MLCK activation and Ca^{2+}-independent SMPP-1M inhibition (16).

Although observations suggest that an abnormal vasocontraction is associated with *PKD/Pkd* mutations, direct evidence is lacking. In this study, the contractile responses of *Pkd2*$^{+/-}$

Received May 19, 2006. Accepted November 13, 2006.

Published online ahead of print. Publication date available at www.jasn.org.

Address correspondence to: Dr. Qi Qian, Department of Medicine and Physiology, Eisenberg S-24, Nephrology, Mayo Clinic College of Medicine, 200 First Street, SW, Rochester, MN 55905. Phone: 507-266-7083; Fax: 507-266-9315; E-mail: qian.qi@mayo.edu

ISSN: 1046-6673/-0001

arteries were examined. De-endothelialized *Pkd2*$^{+/-}$ conduit (thoracic) arteries were found to develop an exaggerated vasocontraction in response to PE stimulation and a left shift in PE dosage-response curve with a significantly reduced PE EC_{50}. Heightened levels of Ca^{2+}-independent force generation and SM contractile protein expression seem to contribute to these abnormalities. Similarly, de-endothelialized *Pkd2*$^{+/-}$ resistance (fourth-order mesenteric) arteries responded to PE with an elevated vasocontraction but a diminished rise in the $[Ca^{2+}]_i$.

Materials and Methods

Animal Genotyping, BP Measurement, and Vessel Preparation

The generation and genotyping of *Pkd2*$^{+/-}$ mice were as reported previously (17). All animal experiments, approved by the Institutional Animal Care and Use Committee, were conducted using congenic male 3- to 5-mo-old wild-type (wt) and *Pkd2*$^{+/-}$ littermates. Systolic BP was measured at the same time of day, with previous 3-d training, using the tail-cuff technique. The average reading from 10 measurements per mouse was taken for analysis. For vessel preparation, an approximately 15-mm portion of descending thoracic aorta was removed from killed mice and placed in chilled Krebs-Ringer Solution (K-R) that contained (in mM) 118 NaCl, 4.7 KCl, 2.5 $CaCl_2$, 1.2 KH_2PO_4, 1.2 $MgSO_4$, 25 $NaHCO_3$, and 10 glucose (pH 7.4) and was aerated with 5% CO_2 in oxygen. The adventitia was excised and endothelium was removed by insertion of a dissecting pin through the lumen and gentle rolling of the vessel on a filter paper that was submerged in K-R. The aortas then were cut into rings or helical strips.

Isometric Force Measurements

Aortic ring (2 mm) was mounted into an organ bath (Radnoti Glass Technology, Monrovia, CA) *via* two stainless steel wires between a stationary rod and a calibrated force transducer (FT-03D; Grass Instruments, Quincy, MA). Aortic helical strip was mounted into a 0.1-ml quart cuvette of a Guth Scientific Instrument Muscle Research System *via* two microforceps, between a force transducer and micromanipulator (described in detail previously [18,19]). The aortic rings were given 1 g of passive tension, and strips were stretched to 150% of their resting length (the optimal tension and length, respectively, determined by preliminary experiments) while superfused (3 to 4 ml/min) with K-R for the rings and HBSS (pH 7.4) for the strips at 37°C, aerated with 5% CO_2 in oxygen. The preparations were maintained at their optimal tension/length throughout the experiments. Endothelium denudation was verified by lacking acetylcholine-induced (10^{-5} M) relaxation in PE (5×10^{-6} M) contracted vessel preparations. The isometric force for both preparations was recorded using Labview 5.0 (National Instruments, Austin, TX).

β-Escin Permeabilization

The aortic strips (1.5 × 5.0 mm) were mounted to the Guth System. After a contractile response to KCl (90 mM) was recording, the strips were permeabilized with β-escin (2×10^{-7} M) in pCa9 solution (×30 min) as described by us previously (19). β-Escin creates pores in the plasma membrane, permitting Ca^{2+} to diffuse freely across. After permeabilization, β-escin was removed by superfusing in pCa9. After being treated with Ca^{2+} ionophore A23187 (10^{-6} M; ×20 min), the strips were stimulated with caffeine (10^{-3} M) to deplete the sarcoplasmic reticulum (SR) Ca^{2+}, verified by lack of contraction to repeated caffeine (10^{-3} M) stimulation (20). The strips then were superfused with pCa9 that contained CaM (10^{-6} M, ×20 min) and stimulated with incremental concentrations of Ca^{2+} (10^{-8} to 10^{-5} M).

Simultaneous Ca^{2+} and Force Measurement in Intact Aortic Helical Strips

Aortic strips (1.0 × 3.0 mm) were mounted on the Guth System, loaded with 5 μM fura 2-AM/0.1% pluronic F-127 in HBSS (×3 h) at their optimal length, superfused in HBSS (37°C, ×20 min) to remove extracellular fura 2-AM, and stimulated with PE (5×10^{-6} M). PE, rather than angiotensin II or vasopressin or thromboxane agonist, was used throughout the study because PE seemed to generate responses with less inter- or intraexperimental variation. The size of the strips was determined on the basis of our preliminary studies that demonstrated an optimal fura 2-AM loading and emission capturing. The fluorescence emission at 510 nm, with 340 and 380 nm excitations by a mercury lamp, was collected by a photomultiplier tube. The emission ratio (R340/380) and force (in mV) were recorded simultaneously. At the end of each experiment, the background fluorescence, the emission at 510 nm with excitation at 360 nm (the isobestic point for fura 2 fluorescence) after the strips were treated with ionomycin (4.0×10^{-6} M × 20 min) followed by $MnCl_2$ (2.0×10^{-3} M × 20 min), was subtracted from the measured emissions. Mn^{2+} rapidly binds to and quenches fura 2 fluorescence, allowing the determination of background fluorescence (21).

Total and Phosphorylated MLC_{20} Measurement

Aortic helical strips, with or without PE (5.0×10^{-6} M) stimulation according to the same protocol as the force measurement, were flash-frozen in dry ice–cooled acetone that contained 10% (wt/vol) trichloroacetic acid and 10 mM dithiothreitol (DTT). The strips then were thawed to room temperature, washed in acetone that contained 10 mM DTT, and air-dried. The dry weight of the strips was 168 to 252 μg. MLC_{20} was extracted at room temperature (×1 h) in buffer that contained 10 mM DTT, 8 M urea, 20 mM Tris base (pH 8.8), and 22 mM glycine, as described previously (22). The ratio of added extraction buffer (μl) to sample weight (μg) was 1:2 (vol/wt). Half of the total extraction from each sample was divided further and subjected to SDS-PAGE in 10% Bis-Tris gel (Dinitrogen, Carlsbad, CA). MLC_{20} was detected by hybridization of electrotransferred nitrocellulose membrane with a polyclonal MLC_{20} antibody. This method does not separate phosphorylated from nonphosphorylated MLC_{20} and thus detects the total MLC_{20}. The other half, also evenly divided, was subjected to urea-glycerol gel electrophoresis to separate phosphorylated MLC_{20} (22). The proteins then were electrotransferred, detected by immunoblottings, and quantified by densitometry using a 300-dpi digital scanner.

PE Stimulation in Pressurized Mesenteric Arteries

The mesenteries from killed mice were removed *en block* into chilled K-R solution. A 3-mm segment of fourth-order mesenteric artery was dissected and cannulated at both ends in a pressure arteriograph and mounted onto the stage of an inverted microscope (TE300; Nikon, Melville, NY). The endothelium was removed by infusion of 0.5 ml of air through the artery. The intraluminal pressure was elevated gradually to 60 mmHg using a servo-controlled pressure system (Living Systems Instrumentation, Burlington, VT). The pressurized arteries then were loaded with 5 μM fura 2-AM (×1 h) followed by superfusion with K-R (37°C) that was aerated with 5% CO_2 in oxygen (×30 min) to remove extracellular fura 2-AM. The arteries then were stimulated with PE (10^{-10} to 10^{-4} M). The fluorescence emission at 510 nm (R340/380)

and the changes of the arterial external diameter, monitored by a video microscopy (IonOptix, Milton, MA), were recorded simultaneously.

Protein Fractionation and Quantitative Western Analysis

Total SM homogenates from the media of aortas were separated by SDS-PAGE, as described previously (23,24). Briefly, SM homogenates (150 ng of protein from each sample) were obtained by grinding, sonicating, and boiling in a sample buffer that contained (in M) 8 urea, 2 thiourea, 0.05 Tris (pH 6.8), 0.7 2β-mercaptoethanol, and 3% SDS and were separated electrophoretically in a 5 to 8% polyacrylamide gradient gel (20 × 40 cm, pH 8.8). The SM MHC were identified by silver staining that showed dominant bands of approximately 200 kD (SM1 and SM2 isoforms as two closely positioned bands) and confirmed by protein sequencing (25) (Mayo Proteomic Research Center). SM α-actin was detected by hybridization of the electrotransferred nitrocellulose membrane with monoclonal SM α-actin antibody (Sigma, St. Louis, MO) (11). The relative expression of SM MHC and α-actin was quantified by densitometry.

α-Actin Immunostaining

Paraffin-embedded aortic sections were deparaffinized in xylene (×12 min), hydrated in ethanol, rinsed in TBS, and blocked in a universal blocking solution (Dako Cytomation, Carpinteria, CA). The sections were stained with SM α-actin antibody or mouse isotype IgG as negative control in antibody diluents at room temperature overnight. The sections then were rinsed in TBS, treated in Envision+(mouse), rinsed again in TBS and deionized water, stained with hematoxylin, dehydrated in ethanol, and mounted for visualization.

Statistical Analyses

All values are expressed as means ± SEM. Comparisons between wt and *Pkd2*$^{+/-}$ arteries were performed using *t* test or two-way ANOVA with Bonferroni *post hoc* analysis. $P < 0.05$ was considered significant.

Results

Pkd2$^{+/-}$ *Mice Show No Evidence of BP Elevation*

Systemic BP was measured in 12 wt and 16 *Pkd2*$^{+/-}$ male littermates, age within 3 to 5 mo, using the tail-cuff method. No significant difference was found (wt 114.5 ± 4.04 *versus Pkd2*$^{+/-}$ 119.33 ± 4.47 mmHg; $P = 0.43$).

Pkd2$^{+/-}$ *Aortic Rings Develop an Exaggerated Vasocontraction to PE Stimulation and a Left Shift in the PE Dosage-Response Curve*

For determination of the agonist-induced vasocontraction, de-endothelialized rings, isolated from the thoracic aortas of male wt and *Pkd2*$^{+/-}$ littermates, were stimulated with incremental concentrations of PE, and PE-induced isometric forces were recorded. Figure 1A shows a representative dosage-response trace of a *Pkd2*$^{+/-}$ aortic ring. Figure 1B depicts the PE-stimulated isometric contraction; *Pkd2*$^{+/-}$ rings responded to PE with a higher maximum force (F_{max}; 5.78 ± 0.73 mN) than that of wt (2.69 ± 0.43 mN; $P < 0.001$) studied in parallel. Furthermore, the PE dosage-response curve of *Pkd2*$^{+/-}$ rings

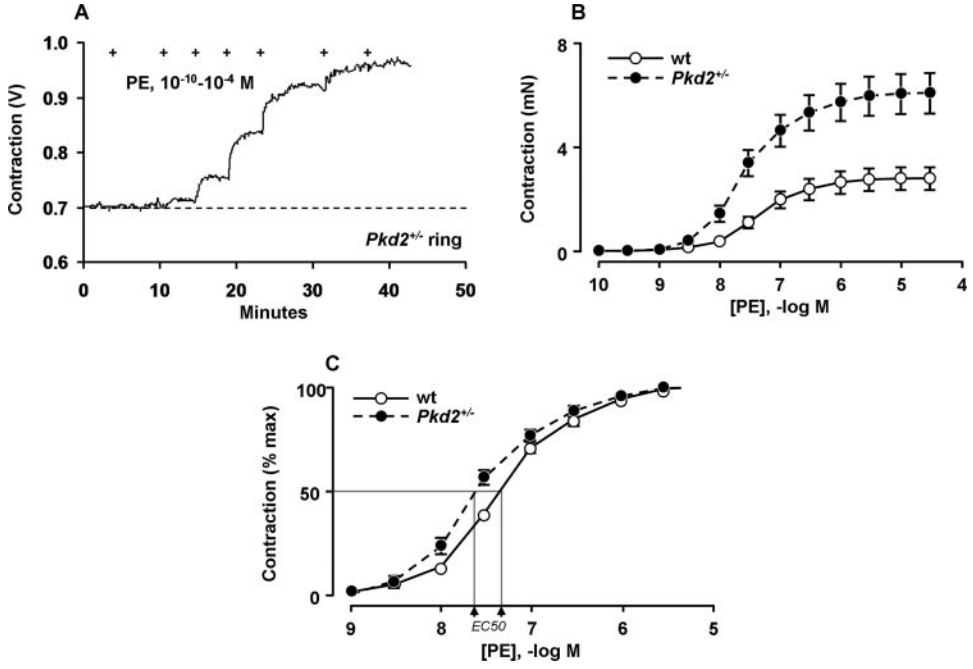

Figure 1. Pkd2$^{+/-}$ have an elevated maximum force (F_{max}; in mN) and a left shift of phenylephrine (PE) dosage-response curve. (A) Representative trace of PE stimulation and corresponding isometric force generation in a *Pkd2*$^{+/-}$ aortic ring. $^{+}$Escalating concentration of PE (10^{-10} to 10^{-4} M). *Y* axis denotes force in volts (V). (B) Isometric contraction generated by incremental concentrations of PE stimulation in wt ($n = 8$, 6 mice) and *Pkd2*+/− ($n = 10$, 5 mice) aortic rings. Contraction is plotted as a function of PE concentration (−log M). The PE dosage-force curves from wild-type (wt) and *Pkd2*$^{+/-}$ rings were compared using two-way ANOVA. *Pkd2*$^{+/-}$ rings generated a higher force than that of wt ($P < 0.001$). (C) The data from B were plotted to show the percentage contraction as a function of PE concentration (−log M). The curve from *Pkd2*$^{+/-}$ rings shifted to the left of that from wt rings. PE EC_{50} is lower in *Pkd2*$^{+/-}$ than that in wt rings.

shifted to the left (Figure 1C) and PE EC_{50} was reduced (60.9 ± 6.2 *versus* 30.4 ± 5.5 nM; $P < 0.001$), indicating an increased sensitivity to PE stimulation.

Pkd2$^{+/-}$ *Aortic SM Strips Generate a Higher Level of Force for a Given Change of* $[Ca^{2+}]_i$ *Responding to PE Stimulation*

To determine the F_{max} for a given level of $[Ca^{2+}]_i$, we examined PE-stimulated changes in force and $[Ca^{2+}]_i$ simultaneously. Using a custom-built Guth system, aortic strips were stretched passively to their optimal length and loaded with fura 2-AM. The changes in isometric force and $[Ca^{2+}]_i$ to PE stimulation (1.0×10^{-5} M) were recorded in real time. As did the aortic rings, *Pkd2*$^{+/-}$ aortic strips developed a higher force (4.31 ± 0.89 *versus* 2.2 ± 0.62 mN; $P = 0.038$; Figure 2, B and C, representative traces in black). However, the rise in $[Ca^{2+}]_i$ was diminished markedly (0.047 ± 0.002 *versus* 0.012 ± 0.003; $P = 0.016$; Figure 2, B and C, traces in red), resulting a higher $\Delta force/\Delta [Ca^{2+}]_i$ ratio than that in wt ($P < 0.001$; Figure 2A). Therefore, in response to PE stimulation, *Pkd2*$^{+/-}$ aortic SM are able to generate a higher force at a given rise of $[Ca^{2+}]_i$.

Pkd2$^{+/-}$ *Aortic SM Strips Generate a Higher Level of Phosphorylated* MLC_{20} *Responding to PE Stimulation*

Because of its key role in force generation, the levels of MLC_{20}, total and phosphorylated, were examined. As shown in Figure 3A, at baseline (time 0), wt and *Pkd2*$^{+/-}$ aortic SM showed similar percentage levels of phosphorylated MLC_{20}. Under maximal PE (1.0×10^{-5} M) stimulation (×3 min, sufficient time for the strips to reach F_{max} on the basis of our observation), *Pkd2*$^{+/-}$ SM generated a higher level of phosphorylated MLC_{20} than those in wt (75.75 ± 5.52 *versus* 56.58 ± 3.33%; $P < 0.01$). Furthermore, the total level of MLC_{20}, quantified by densitometric analyses of the Western blots hybridized with polyclonal MLC_{20} antibody, was elevated significantly in *Pkd2*$^{+/-}$ than in wt aortic SM ($82.75 \pm 2.94 \times 10^3$ *versus* $73 \pm 2.09 \times 10^3$; $P = 0.03$). The representative blots of the total and phosphorylated MLC_{20} are shown in Figure 3B.

Pkd2$^{+/-}$ *and wt Aortic SM Have a Similar pCa Percentage Force Relationship*

We reasoned that an elevated vasocontraction with a diminished rise in $[Ca^{2+}]_i$ in *Pkd2*$^{+/-}$ arteries might result from a heightened sensitivity of CaM/MLCK/force generation to Ca^{2+}, which would shift the pCa-force curve (15,26–28). To study the pCa^{2+}–force relationship, de-endothelialized aortic helical strips were permeabilized with β-escin using an established protocol (29) and stimulated with Ca^{2+} (pCa8-5). β-Escin was chosen because it permeabilizes the plasma membrane more completely in this full-thickness preparation than α toxin (Q.Q., preliminary observations). Because contractile proteins and MLCK are not detergent extractable, β-escin permeabilization ensures a synchronized exposure of contractile proteins to known concentrations of Ca^{2+} without compromising contraction. Forces were elicited at pCa 6.7 to 5.0; F_{max} was reached at pCa approximately 5.5 for both wt and *Pkd2*$^{+/-}$ strips. The pCa-force curves were superimposable (Figure 4A), indicating that similar levels of CaM/MLCK activity were elicited at given concentrations of Ca^{2+}. Therefore, compared with that in wt, the Ca^{2+}-dependent CaM/MLCK pathway in *Pkd2*$^{+/-}$ aortic SM was not more sensitive to Ca^{2+}.

Although the pCa-force curves were nearly identical, a significant difference in the absolute F_{max} was detected. *Pkd2*$^{+/-}$ strips developed a higher F_{max} (0.624 ± 0.06 mN) than that in wt (0.456 ± 0.07 mN; $P < 0.01$; Figure 4B). A higher F_{max} without a shift of pCa-force curve suggests that the difference in F_{max} could be distal to Ca^{2+}/CaM/MLCK and might be related to a different level of contractile protein expression in wt and *Pkd2*$^{+/-}$ arteries.

It should be noted that the F_{max} that was elicited from this group of experiments cannot be compared numerically with the F_{max} from the aortic ring studies. This is because the orientations of VSMC are not the same between the two preparations; neither were the stimulants: The permeabilized strips were stimulated by Ca^{2+}, whereas the rings were evaluated by PE.

Pkd2$^{+/-}$ *Aortas Contain Elevated Levels of Contractile Proteins*

Previously, in the course of quantifying polycystin-2 (the protein product of *Pkd2*), we noted that SM α-actin tended to be higher in *Pkd2*$^{+/-}$ VSMC (11). This previous finding plus the finding of a higher Ca^{2+}-induced F_{max} suggests an altered level of contractile protein expression in *Pkd2*$^{+/-}$ VSMC. As shown in Figure 5A, quantitative Western analyses of aortic SM homogenates that were isolated from five pairs of littermates

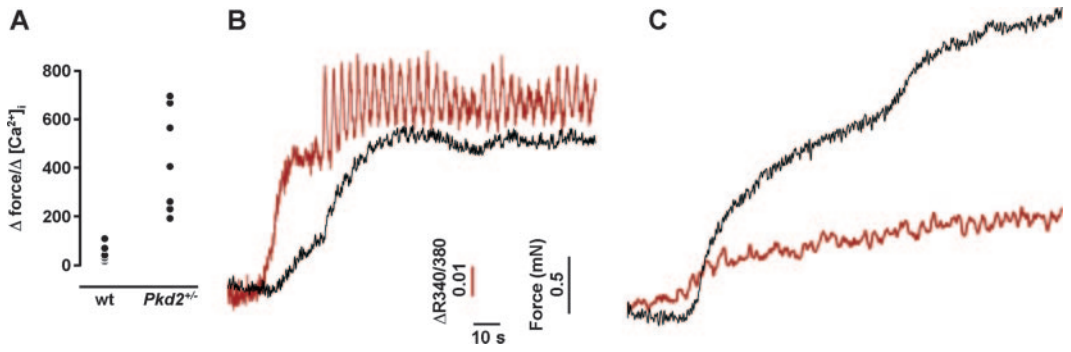

Figure 2. (A) PE induced a much larger $\Delta force/\Delta Ca^{2+}$ ratio in *Pkd2*$^{+/-}$ aortic strips ($n = 7$, 6 mice) than in wt ($n = 7$, 5 mice). (B and C) Representative traces of simultaneously recorded $[Ca^{2+}]_i$ (red) and force (black) changes in response to PE (5×10^{-6} M) stimulation in wt (B) and *Pkd2*$^{+/-}$ (C) strips.

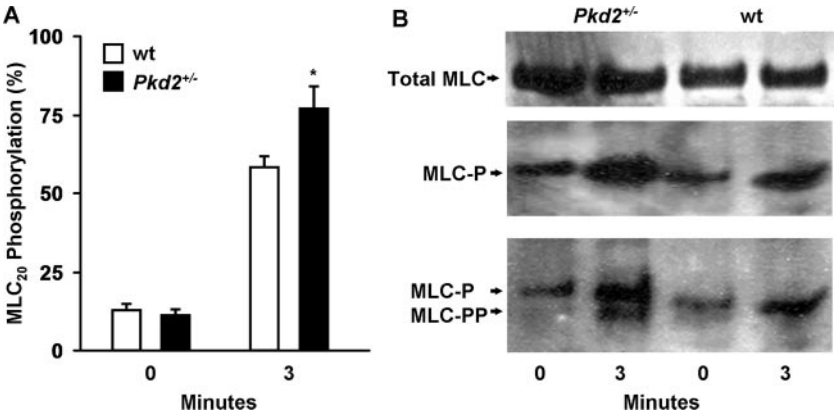

Figure 3. (A) The percentage of phosphorylated MLC_{20} is expressed as the density of mono- and diphosphorylated MLC_{20} bands divided by the density of the total MLC_{20} bands. At time 0, wt and *Pkd2*$^{+/-}$ showed a similar percentage level of MLC_{20} phosphorylation. With 3 min of PE (5×10^{-6} M) stimulation, *Pkd2*$^{+/-}$ strips generated a higher percentage level of phosphorylated MLC_{20} ($n = 4$ wt and four *Pkd2*$^{+/-}$ mice, at each time point). (B) Representative immunoblots from quantitative Western analyses showing the total MLC_{20} (top) detected by a polyclonal MLC_{20} antibody (FL-172, sc-15370) and phosphorylated MLC_{20} (middle) separated by 8 M urea-glycerol gel and detected by a antiphosphoserine antibody (Chemicon AB1603), and the blot (from the middle) was stripped and reprobed with anti-Thr18 and Ser19 phosphorylated MLC_{20} (Santa Cruz sc-12896; bottom). *Pkd2*$^{+/-}$ strip showed a higher level of phosphorylated MLC_{20} after PE stimulation.

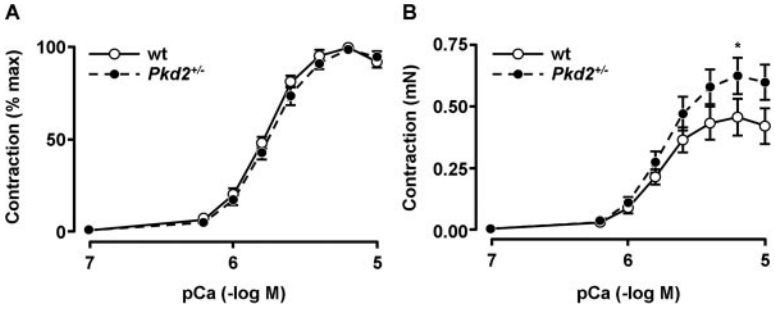

Figure 4. (A) pCa-force curves in wt ($n = 5$, 5 mice) and *Pkd2*$^{+/-}$ ($n = 6$, 6 mice) strips plotted to show the percentage contraction as a function of Ca^{2+} concentration (pCa in $-$log M). (B) The same data presented as the contraction in mN as a function of pCa. *$P < 0.01$, significant difference in F_{max} between the wt and *Pkd2*$^{+/-}$ strips.

showed that *Pkd2*$^{+/-}$ SM expressed a higher level of SM α-actin ($61.89 \pm 7.69 \times 10^3$ *versus* $46.34 \pm 4.68 \times 10^3$; $P = 0.01$). This finding was verified by direct SM α-actin immunostaining of the cross-sections of aortas. Although much less quantitative, the staining of three pairs of aortas from wt and *Pkd2*$^{+/-}$ littermates showed the same trend. Representative pictures are shown in Figure 5, C and D. Total MHC expression was quantified by electrophoretic separation of aortic SM homogenates, which generated prominent bands that could be visualized by silver stain (150 ng of protein loading) at approximately 200 and 42 kD, consistent with SM MHC and α-actin (23,24,30). The protein sequence–verified MHC (SM1 and SM2 isoforms) on a silver-stained SDS-PAGE gel are shown (Figure 5B). *Pkd2*$^{+/-}$ SM contained a higher level of total SM MHC ($4.61 \pm 0.16 \times 10^3$) than that in wt ($3.98 \pm 0.18 \times 10^3$; $P = 0.037$).

Pkd2$^{+/-}$ *Resistance Arteries Develop an Exaggerated PE-Induced Vasocontraction with a Diminished Rise in* $[Ca^{2+}]_i$

To examine the contractile response in resistance arteries, we built a minivessel system that allowed simultaneous recording of changes in isotonic vasocontraction and $[Ca^{2+}]_i$ (Figure 6A). Fourth-order de-endothelialized mesenteric arteries (external diameter of 200 to 240 μm) from male wt or *Pkd2*$^{+/-}$ littermates were mounted, pressurized (60 mmHg), loaded with fura 2-AM, and stimulated with PE. Figure 6B shows representative traces of the simultaneously recorded changes in the external arterial diameter (representing isotonic contraction) and corresponding increases in $[Ca^{2+}]_i$ in a wt mesenteric artery. At each PE concentration, the maximal change in $[Ca^{2+}]_i$ and a sustained change in diameter were used for analysis. As shown in Figure 7B, *Pkd2*$^{+/-}$ arteries elevated $[Ca^{2+}]_i$ by approximately half of that in wt. Despite the difference in $[Ca^{2+}]_i$, *Pkd2*$^{+/-}$ mesenteric arteries, as did aortas, generated a higher level of contraction than that in wt ($P < 0.001$; Figure 7A).

Discussion

The exaggerated vasocontraction in *Pkd2*$^{+/-}$ arteries that was induced by PE is reminiscent of arterial vasospasms that were observed in ADPKD (4,5). The absence of hypertension in mice

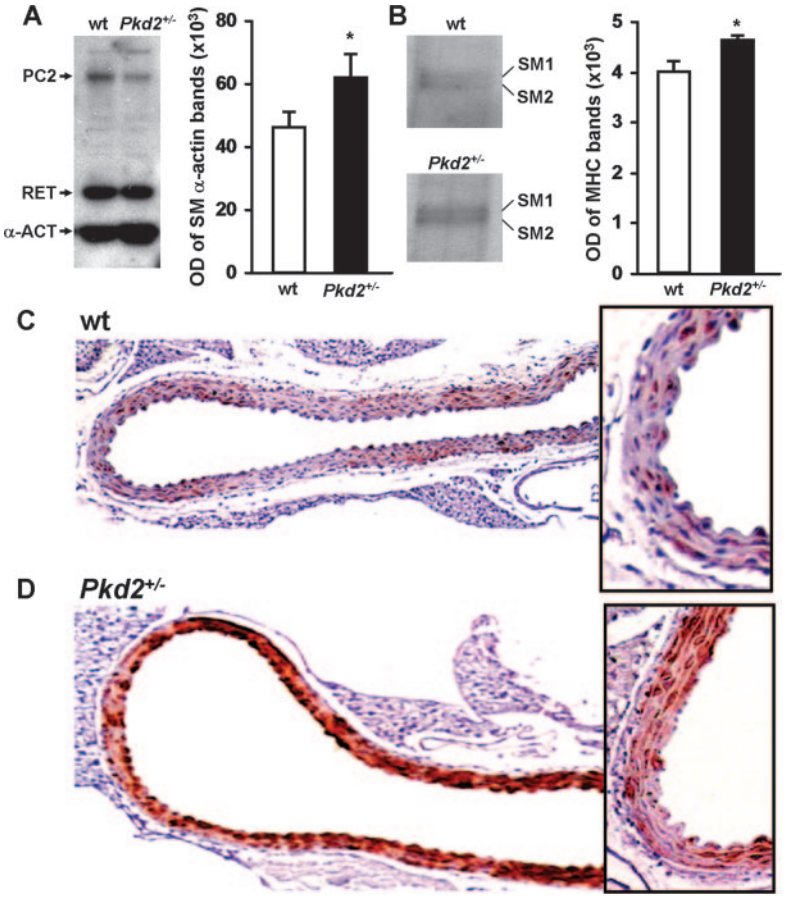

Figure 5. (A) Representative quantitative Western blot (left) and densitometric analysis (right) of smooth muscle (SM) α-actin, showing *Pkd2*$^{+/-}$ vascular SM have a reduced polycystin-2 (PC2) expression and an elevated SM α-actin (α-ACT) expression (n = 5; $P < 0.01$ *versus* wt). Calreticulin (RET) shows equal protein loading. (B left) Representative silver-stained gels showing the electrophoretically separated myosin heavy chain (MHC) isoforms (SM1 and SM2). (Right) Densitometric analysis of SM MHC quantification showing an elevated SM MHC expression in *Pkd2*$^{+/-}$ SM (n = 7; P = 0.03 *versus* wt). (C and D) Representative immunostaining of SM α-actin in wt (C) and *Pkd2*$^{+/-}$ (D) aortas. Inserts show enlarged pictures of the same sections.

with which the vasocontractile function was studied eliminates possible confounding factors in force generation, including alterations in SM internal load and stiffness (12,31,32). However, our previous observations of reduced SR Ca^{2+} store and basal $[Ca^{2+}]_i$ in *Pkd2*$^{+/-}$ VSMC would not have predicted these results. This dilemma was addressed by concomitant examination of the PE-induced vasocontraction and the change in $[Ca^{2+}]$i. We found (Figure 2) that *Pkd2*$^{+/-}$ aortic strips developed a higher force associated with a higher level of phosphorylated MLC_{20} (Figure 3) yet a diminished rise in $[Ca^{2+}]_i$. These observations thus confirm the results from PE-stimulated aortic ring preparations (Figure 1) and our previous finding of $[Ca^{2+}]_i$ derangements in single *Pkd2*$^{+/-}$ VSMC (11).

PE selectively activates α1-AR, $G_{\alpha q/11}$ protein–coupled receptors ($G_{\alpha q/11}$PCR). α1-AR activation induces MLC_{20} phosphorylation and vasocontraction by activating Ca^{2+}-dependent MLCK and Ca^{2+}-independent PKC and Rho/ROK kinases, which, in turn, inhibit MLC_{20} de-phosphorylation (26,28,33). We considered two possibilities for the exaggerated PE-induced vasocontraction in *Pkd2*$^{+/-}$ arteries. The first possibility is that CaM/MLCK in *Pkd2*$^{+/-}$ VSMC are abnormally sensitive to $[Ca^{2+}]_I$ and thereby capable of being fully activated at a lower level of $[Ca^{2+}]_i$. The second possibility is that CaM/MLCK activity is unaltered but rather the Ca^{2+}-independent signaling functions at a higher level. If the former is correct, then a left shift of the pCa-force curve in *Pkd2*$^{+/-}$ vessels to that in wt would be observed. If the pCa–force relationship is unaltered, then hyperfunction of the Ca^{2+}-independent mechanisms likely would exist and account for the observed abnormalities.

These possibilities were dissected by separating the Ca^{2+}-stimulated effect from the α1-AR–mediated signaling. β-Escin permeabilized aortic strips were stimulated by Ca^{2+} alone. As shown in Figure 4A, when α1-AR was unstimulated, Ca^{2+} did not shift the pCa-force curve in *Pkd2*$^{+/-}$ strips, indicating that CaM/MLCK in both types of arteries displayed a similar sensitivity to Ca^{2+}. The left shift of the PE dosage-response curve and elevated $\Delta force/\Delta[Ca^{2+}]_i$ in *Pkd2*$^{+/-}$ strips likely resulted from a heightened, α1-AR–mediated Ca^{2+}-independent signaling.

Although the absolute levels vary, a similar pattern of force/$[Ca^{2+}]_i$ abnormalities was elicited by PE stimulation in *Pkd2*$^{+/-}$ resistance (fourth-order mesenteric) arteries (Figure 7). The dif-

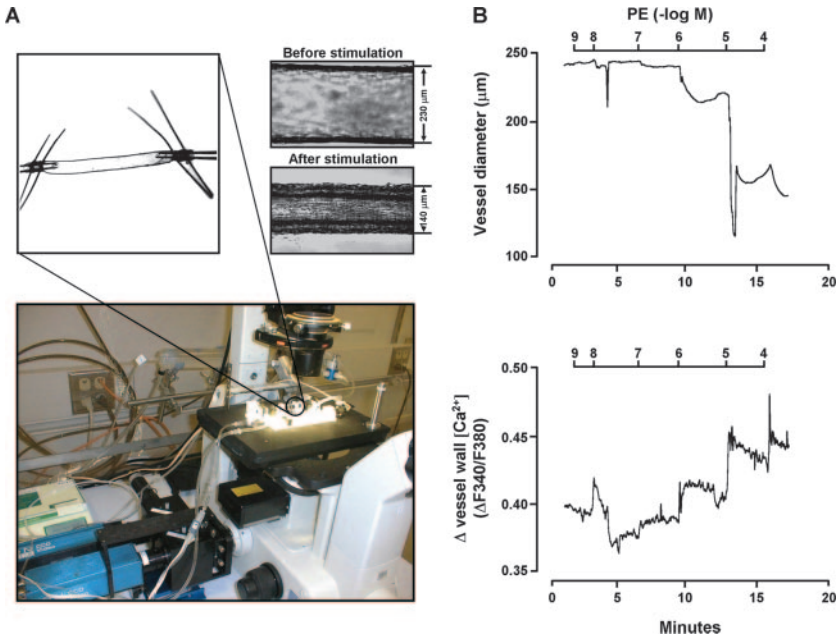

Figure 6. (A) Minivessel system. Top left shows two ends of the fourth-order mesenteric arteries connected to glass cannulas in an arteriograph positioned on an inverted microscope (bottom left). Top right shows the change in the external diameters of mesenteric arteries before and after PE stimulation. (B) Representative traces of the changes in the external diameter of the artery (top) and corresponding changes in $[Ca^{2+}]_i$ (bottom) with PE stimulation.

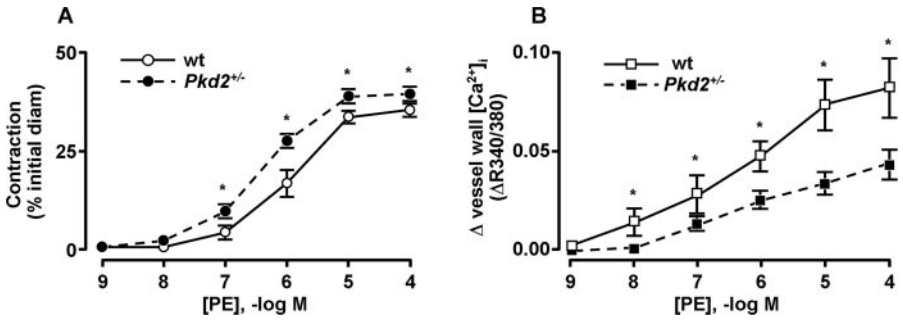

Figure 7. (A) The change in percentage of external diameter of the mesenteric arteries, representing the isotonic vasocontractions, is plotted as a function of PE concentration (−log M). The pressurized *Pkd2*$^{+/-}$ arteries ($n = 6$, 6 mice) developed a higher level of contraction that in wt arteries ($n = 5$, 5 mice) arteries ($P < 0.001$) (B) Simultaneously recorded changes in fura 2 fluorescence emission, representing the changes in the $[Ca^{2+}]_i$, is plotted as a function of PE concentration (−log M), showing that *Pkd2*$^{+/-}$ arteries had a lesser $[Ca^{2+}]_i$ elevation ($P < 0.001$). *Significant difference between the two data sets.

ference in the magnitude of force alteration between *Pkd2*$^{+/-}$ aortic and mesenteric arteries was not unexpected, because agonist-induced force is an integrated output of multiple determinants (31,34). In a given genotype, determinants vary between conduit and resistance arteries, including the shape and geometry of VSMC, the number of focal attachments (dense plaque and dense bands), the α1-AR densities (34), the dynamic cytoskeleton rearrangement during force generation (31), and the amount of contractile proteins (32). Therefore, PE-induced force may not be altered to the same degree. However, a similar pattern of contractile abnormality in both arterial beds suggests a common underlying mechanism(s) and suggests an overall functional abnormality in *Pkd2*$^{+/-}$ arteries.

Exactly how this aberrant vasocontractile response to PE might relate to *Pkd* mutation is beyond the scope of our data. Nevertheless, the consensus on the functions of polycystins offers the following possibilities. Polycystin-1 constitutively activates GPCR, including α_q-coupled receptors (35); polycystin-2 inhibits polycystin-1–mediated GPCR signaling (36). It is tempting to speculate that a reduced polycystin-2 in *Pkd2*$^{+/-}$ VSMC (11) might limit the polycystin-2–mediated inhibition, thereby heightening the GPCR signaling. Alternatively, the Ca^{2+} derangements as a result of *Pkd2*$^{+/-}$ mutation (also observed in ADPKD renal cells [37,38]), might alter the receptor desensitization because PE stimulation–induced α1-AR desensitization/internalization is a Ca^{2+}-dependent process (39,40). Although our data are consistent with these possibilities, other yet-to-be-identified mechanisms cannot be excluded.

The elevated contractile protein expression in *Pkd2*$^{+/-}$ VSMC is a novel finding that merits further investigation. We speculate that such elevated expression may be linked to the $[Ca^{2+}]_i$ dysregulation. Reduction in $[Ca^{2+}]_i$ can promote actin polymerization by interfering with the function of Ca^{2+}-sensitive actin-capping/severing proteins (41–43); excess actin polymerization increases the release of myocardin (an SM transcription factor) from globular actins. Myocardin promotes the expression of a number of SM proteins, including SM α-actin and MHC (44). Given the $[Ca^{2+}]_i$ dysregulation that was observed in *Pkd2*$^{+/-}$ VSMC, it is possible that the altered contractile protein expression may be linked to an altered $[Ca^{2+}]_i$ homeostasis.

In addition to the $[Ca^{2+}]_i$ dysregulation, quiescent *Pkd2*$^{+/-}$ VSMC show approximately two-fold elevation in cAMP (45). cAMP is known (in some cellular systems) to decrease SR Ca^{2+} release (46) and Rho/ROK-mediated SMPP-1M inhibition (47). Therefore, in unstressed conditions, cAMP and $[Ca^{2+}]_i$ dysregulation are expected to restrain contraction in *Pkd2*$^{+/-}$ VSMC. In this regard, impaired visceral SM function that was observed in *Pkd2* mutant drosophila (although cAMP level was not given) could be relevant (48). In our study, however, such considerations likely are overwhelmed by the dominant α1-AR signaling that was provoked by acute PE stimulation.

Conclusion

We demonstrate that *Pkd2*$^{+/-}$ arterial SM exhibit an increased sensitivity and exaggerated contraction to α1-AR agonist stimulation as a result, in part, of significant elevations in agonist-mediated, Ca^{2+}-independent force generation and SM contractile protein expression. These defects may underlie the recognized predisposition to assorted vascular diseases that are associated with *Pkd* mutation.

Acknowledgments

This study was supported by National Institutes of Health grants DK63064 and DK073567 (Q.Q.) and HLO74309 (G.C.S.), Polycystic Kidney Disease Foundation grant 41A2R (Q.Q.), and Mayo Clinic Research Career Development Award (FUTR) (Q.Q.).

Disclosures.

None.

References

1. Torres V, Holley K, Offord K: Epidemiology. In: *Problems in Diagnosis and Management of Polycystic Kidney Disease*, edited by Grantham J, Gardner K, Kansas City, PKR Foundation, 1985, pp 49–69
2. Schacht F: *Hypertension and Vascular Studies in Congenital Polycystic Kidney* [master's thesis], St. Paul, University of Minnesota, 1930
3. King BF, Torres VE, Brummer ME, Chapman AB, Bae KT, Glockner JF, Arya K, Felmlee JP, Grantham JJ, Guay-Woodford LM, Bennett WM, Klahr S, Hirschman GH, Kimmel PL, Thompson PA, Miller JP: Magnetic resonance measurements of renal blood flow as a marker of disease severity in autosomal-dominant polycystic kidney disease. *Kidney Int* 64: 2214–2221, 2003
4. Gabow PA, Ikle DW, Holmes JH: Polycystic kidney disease: Prospective analysis of nonazotemic patients and family members. *Ann Intern Med* 101: 238–247, 1984
5. Chapman AB, Rubinstein D, Hughes R, Stears JC, Earnest MP, Johnson AM, Gabow PA, Kaehny WD: Intracranial aneurysms in autosomal dominant polycystic kidney disease. *N Engl J Med* 327: 916–920, 1992
6. Cai Y, Maeda Y, Cedzich A, Torres VE, Wu G, Hayashi T, Mochizuki T, Park JH, Witzgall R, Somlo S: Identification and characterization of polycystin-2, the PKD2 gene product. *J Biol Chem* 274: 28557–28565, 1999
7. Boulter C, Mulroy S, Webb S, Fleming S, Brindle K, Sandford R: Cardiovascular, skeletal, and renal defects in mice with a targeted disruption of the Pkd1 gene. *Proc Natl Acad Sci U S A* 98: 12174–12179, 2001
8. Loghman-Adham M, Soto CE, Shen X, Zhou J: Mice with targeted mutations in PK1del34/+, develop salt sensitive hypertension [Abstract]. *J Am Soc Nephrol* 12: A2797, 2001
9. Lantinga-van Leeuwen IS, Dauwerse JG, Baelde HJ, Leonhard WN, van de Wal A, Ward CJ, Verbeek S, Deruiter MC, Breuning MH, de Heer E, Peters DJ: Lowering of Pkd1 expression is sufficient to cause polycystic kidney disease. *Hum Mol Genet* 13: 3069–3077, 2004
10. Wu G, Markowitz GS, Li L, D'Agati VD, Factor SM, Geng L, Tibara S, Tuchman J, Cai Y, Park JH, van Adelsberg J, Hou H Jr, Kucherlapati R, Edelmann W, Somlo S: Cardiac defects and renal failure in mice with targeted mutations in Pkd2. *Nat Genet* 24: 75–78, 2000
11. Qian Q, Hunter LW, Li M, Marin-Padilla M, Prakash YS, Somlo S, Harris PC, Torres VE, Sieck GC: Pkd2 haploinsufficiency alters intracellular calcium regulation in vascular smooth muscle cells. *Hum Mol Genet* 12: 1875–1880, 2003
12. Stephens NL, Seow CY, Halayko AJ, Jiang H: The biophysics and biochemistry of smooth muscle contraction. *Can J Physiol Pharmacol* 70: 515–531, 1992
13. Niiro N, Ikebe M: Zipper-interacting protein kinase induces Ca2+-free smooth muscle contraction via myosin light chain phosphorylation. *J Biol Chem* 276: 29567–29574, 2001
14. Wilson DP, Sutherland C, Borman MA, Deng JT, Macdonald JA, Walsh MP: Integrin-linked kinase is responsible for Ca2+-independent myosin diphosphorylation and contraction of vascular smooth muscle. *Biochem J* 392: 641–648, 2005
15. Somlyo AP, Somlyo AV: Signal transduction through the RhoA/Rho-kinase pathway in smooth muscle. *J Muscle Res Cell Motil* 25: 613–615, 2004
16. Walsh MP, Horowitz A, Clement-Chomienne O, Andrea JE, Allen BG, Morgan KG: Protein kinase C mediation of Ca2+-independent contractions of vascular smooth muscle. *Biochem Cell Biol* 74: 485–502, 1996
17. Wu G, D'Agati V, Cai Y, Markowitz G, Park JH, Reynolds DM, Maeda Y, Le TC, Hou H Jr, Kucherlapati R, Edelmann W, Somlo S: Somatic inactivation of Pkd2 results in polycystic kidney disease. *Cell* 93: 177–188, 1998
18. Guth K, Wojciechowski R: Perfusion cuvette for the simultaneous measurement of mechanical, optical and energetic parameters of skinned muscle fibres. *Pflugers Arch* 407: 552–557, 1986
19. Sieck GC, Han YS, Pabelick CM, Prakash YS: Temporal

aspects of excitation-contraction coupling in airway smooth muscle. *J Appl Physiol* 91: 2266–2274, 2001
20. Garcia FC, Stiffel VM, Pearce WJ, Zhang L, Gilbert RD: Ca2+ sensitivity of fetal coronary arteries exposed to long-term, high-altitude hypoxia. *J Soc Gynecol Investig* 7: 161–166, 2000
21. Pabelick CM, Rehder K, Jones KA, Shumway R, Lindahl SG, Warner DO: Stereospecific effects of ketamine enantiomers on canine tracheal smooth muscle. *Br J Pharmacol* 121: 1378–1382, 1997
22. Gunst SJ, al-Hassani MH, Adam LP: Regulation of isotonic shortening velocity by second messengers in tracheal smooth muscle. *Am J Physiol* 266: C684–C691, 1994
23. Han YS, Proctor DN, Geiger PC, Sieck GC: Reserve capacity for ATP consumption during isometric contraction in human skeletal muscle fibers. *J Appl Physiol* 90: 657–664, 2001
24. Yates LD, Greaser ML: Quantitative determination of myosin and actin in rabbit skeletal muscle. *J Mol Biol* 168: 123–141, 1983
25. Hasegawa K, Arakawa E, Oda S, Matsuda Y: Molecular cloning and expression of murine smooth muscle myosin heavy chains. *Biochem Biophys Res Commun* 232: 313–316, 1997
26. Singer HA: Protein kinase C activation and myosin light chain phosphorylation in 32P-labeled arterial smooth muscle. *Am J Physiol* 259: C631–C639, 1990
27. Seto M, Sasaki Y: Stimulus-specific patterns of myosin light chain phosphorylation in smooth muscle of rabbit thoracic artery. *Pflugers Arch* 415: 484–489, 1990
28. Colburn JC, Michnoff CH, Hsu LC, Slaughter CA, Kamm KE, Stull JT: Sites phosphorylated in myosin light chain in contracting smooth muscle. *J Biol Chem* 263: 19166–19173, 1988
29. Kannan MS, Fenton AM, Prakash YS, Sieck GC: Cyclic ADP-ribose stimulates sarcoplasmic reticulum calcium release in porcine coronary artery smooth muscle. *Am J Physiol* 270: H801–H806, 1996
30. Weber LP, Van Lierop JE, Walsh MP: Ca2+-independent phosphorylation of myosin in rat caudal artery and chicken gizzard myofilaments. *J Physiol* 516: 805–824, 1999
31. Meiss R: An analysis of length-dependent stiffness in smooth muscle strips. In: *Regulation of Smooth Muscle*, edited by RM, New York, Plenum, 1991, pp 425–434
32. Murphy RA, Herlihy JT, Megerman J: Force-generating capacity and contractile protein content of arterial smooth muscle. *J Gen Physiol* 64: 691–705, 1974
33. Gokina NI, Osol G: Temperature and protein kinase C modulate myofilament Ca2+ sensitivity in pressurized rat cerebral arteries. *Am J Physiol* 274: H1920–H1927, 1998
34. Rudner XL, Berkowitz DE, Booth JV, Funk BL, Cozart KL, D'Amico EB, El-Moalem H, Page SO, Richardson CD, Winters B, Marucci L, Schwinn DA: Subtype specific regulation of human vascular alpha(1)-adrenergic receptors by vessel bed and age. *Circulation* 100: 2336–2343, 1999
35. Parnell SC, Magenheimer BS, Maser RL, Zien CA, Frischauf AM, Calvet JP: Polycystin-1 activation of c-Jun N-terminal kinase and AP-1 is mediated by heterotrimeric G proteins. *J Biol Chem* 277: 19566–19572, 2002
36. Delmas P, Nomura H, Li X, Lakkis M, Luo Y, Segal Y, Fernandez-Fernandez JM, Harris P, Frischauf AM, Brown DA, Zhou J: Constitutive activation of G-proteins by polycystin-1 is antagonized by polycystin-2. *J Biol Chem* 277: 11276–11283, 2002
37. Aguiari G, Banzi M, Gessi S, Cai Y, Zeggio E, Manzati E, Piva R, Lambertini E, Ferrari L, Peters DJ, Lanza F, Harris PC, Borea PA, Somlo S, Del Senno L: Deficiency of polycystin-2 reduces Ca2+ channel activity and cell proliferation in ADPKD lymphoblastoid cells. *FASEB J* 18: 884–886, 2004
38. Yamaguchi T, Hempson SJ, Reif GA, Hedge AM, Wallace DP: Calcium restores a normal proliferation phenotype in human polycystic kidney disease epithelial cells. *J Am Soc Nephrol* 17: 178–187, 2006
39. Minneman KP: alpha1-Adrenergic receptor subtypes, inositol phosphates, and sources of cell Ca2+. *Pharmacol Rev* 40: 87–119, 1988
40. Hieble JP, Bylund DB, Clarke DE, Eikenburg DC, Langer SZ, Lefkowitz RJ, Minneman KP, Ruffolo RR Jr: International Union of Pharmacology. X. Recommendation for nomenclature of a 1-adrenoceptors: Consensus update. *Pharmacol Rev* 47: 267–270, 1995
41. Burtnick LD, Koepf EK, Grimes J, Jones EY, Stuart DI, McLaughlin PJ, Robinson RC: The crystal structure of plasma gelsolin: Implications for actin severing, capping, and nucleation. *Cell* 90: 661–670, 1997
42. Kumar N, Tomar A, Parrill AL, Khurana S: Functional dissection and molecular characterization of calcium-sensitive actin-capping and actin-depolymerizing sites in villin. *J Biol Chem* 279: 45036–45046, 2004
43. Lin KM, Mejillano M, Yin HL: Ca2+ regulation of gelsolin by its C-terminal tail. *J Biol Chem* 275: 27746–27752, 2000
44. Wang Z, Wang DZ, Pipes GC, Olson EN: Myocardin is a master regulator of smooth muscle gene expression. *Proc Natl Acad Sci U S A* 100: 7129–7134, 2003
45. Kip SN, Hunter LW, Ren Q, Harris PC, Somlo S, Torres VE, Sieck GC, Qian Q: [Ca2+]i reduction increases cellular proliferation and apoptosis in vascular smooth muscle cells. Relevance to the ADPKD phenotype. *Circ Res* 96: 873–880, 2005
46. Ding KH, Husain S, Akhtar RA, Isales CM, Abdel-Latif AA: Inhibition of muscarinic-stimulated polyphosphoinositide hydrolysis and Ca2+ mobilization in cat iris sphincter smooth muscle cells by cAMP-elevating agents. *Cell Signal* 9: 411–421, 1997
47. Wooldridge AA, MacDonald JA, Erdodi F, Ma C, Borman MA, Hartshorne DJ, Haystead TA: Smooth muscle phosphatase is regulated in vivo by exclusion of phosphorylation of threonine 696 of MYPT1 by phosphorylation of serine 695 in response to cyclic nucleotides. *J Biol Chem* 279: 34496–34504, 2004
48. Gao Z, Joseph E, Ruden DM, Lu X: Drosophila Pkd2 is haploid-insufficient for mediating optimal smooth muscle contractility. *J Biol Chem* 279: 14225–14231, 2004